Journal of Optoelectronicsand Advanced Materials Vol. 7, No. 4, August 2005, p. 1847 - 1858

DEFECTS INDUCED BY ELECTRON IRRADIATION IN CdSe THIN FILMS

L. Ion, V. A. Antohe, S. Antohe*

University of Bucharest, Faculty of Physics, P.O.Box: MG-11, Bucharest-Magurele, 077125 Romania

Thin films of $A^{II}B^{VI}$ compounds are potential candidates for the manufacturing of electronic and optoelectronic devices, especially solar cells. In this paper the effects of irradiation with high-energy electrons on structural and electrical properties of CdSe thin films have been investigated. The films, 30 μm thick, were prepared by thermal-vacuum evaporation on glass substrate at a temperature of 220 °C. The samples were irradiated with 6-MeV electrons, up to a fluency of 10^{14} e/cm^2. XRD investigation has revealed that the films contain wurtzite-type CdSe, (001) preferentially oriented in the growth direction. The defects induced by electron irradiation have been studied using the Space Charge Limited Currents (SCLC) measurements and Thermally Stimulated Currents (TSC) spectroscopy. It was found that the electrical conduction of the samples, both before and after irradiation, is mainly controlled by a defect having an energy level located at 0.38 eV below the conduction band edge, its density was significantly increased as a result of irradiation. The possible origin of this defect is discussed.

(Received July 12, 2005; accepted July 21, 2005)

Keywords: CdSe, Thin films, Electron irradiation, Defects

1. Introduction

$A^{II}B^{VI}$ compounds are good candidates for practical applications like solar cells, optical detectors and optoelectronic devices. Among them, cadmium sellenide (CdSe) is recommended by a suitable band gap and optical properties as a very promising material for optoelectronic applications like solar cell structures. It is a well-established fact that the performance of the devices based on thin films strongly depends on structural and electronic properties of the films obtained under various experimental conditions. Therefore, the task to identify and to learn how to control the defects having the most important influence on electrical and/or optical properties of the films is very important. Many reports have been published on the electrical properties of vacuum deposited films of CdSe [1-5]. However, little work was done on the influence of the ionizing radiations on their physical properties [6-8]. Given that thin films of A^{II}-B^{VI} compounds, especially CdS, CdSe, CdTe, ZnSe, are potential candidates for producing solar cells used in space technology applications, where the flux of ionizing radiations is high enough, such a study is very important. Irradiation with electrons having energies in MeV range can also be used to investigate simple defects, like vacancies or interstitials, because in this case no massive structural damage is produced. An electron with energy of 1-10 MeV can only produce a small number of atomic displacements [9]. In this paper we present the results of a complex investigation of the changes induced by electron irradiation on the electrical properties of CdSe thin films. Different experimental techniques were used (TSC and SCLC measurements) and the results are discussed. The possible origin of the main defects created by 6-MeV electron is also discussed.

* Corresponding author: santohe@solid.fizica.unibuc.ro

2. Experimental procedures

CdSe thin films, 30 μm thick, were prepared by thermal vacuum evaporation from a single source onto an optical glass substrate. The pressure in the evaporation cell was kept below 2×10^{-5} Torr during the deposition of the films. The evaporator consisted of a quartz container heated to 750 °C, the substrate being maintained at 220°C during the deposition. To improve the structural and chemical homogeneity of the films, they were subsequently thermally treated in vacuum at 300 °C, for 10 min.

Electrical investigations were performed on two types of structures, having respectively gold contacts in a sandwich geometry Au/CdSe/Au and aluminium contacts in a planar geometry. The Au/CdSe/Au sandwich structures were prepared as follows: first a gold strip of 8 mm length, 2 mm width and 300 nm thickness was deposited on a glass plate substrate, then the CdSe film was grown on the gold electrode and, finally, a second gold strip was deposited on the CdSe layer, having the same geometry as the first one but being placed in a perpendicular direction with respect to it. The effective area, formed by the overlap of the electrodes was 0.04 cm^2, of about one order of magnitude smaller than the area of CdSe film to prevent the edge effects. To improve the stability and ohmicity of the contacts, the structures were thermally treated in air at 250 °C, for 30 min. It is known [10,11] that the gold electrodes prepared in this way guarantee stable and relatively good ohmic contacts on CdSe thin films.

Planar structures were prepared by evaporating four Al contacts on top of CdSe films. The contacts, 1 mm×1 mm in surface, 0.3 μm thick and separated by 1 mm, were placed in line.

The obtained structures were subjected to irradiation with electrons supplied by a betatron. The samples were irradiated at room temperature with 6-MeV and 7-MeV electrons to a fluence of 10^{15} electrons/cm^2, irradiation direction being perpendicular to the surface of the samples. The thermal effect during irradiation was negligible.

The structure of the samples was investigated, before and after irradiation, with a θ-2θ X-ray diffractometer, using Cu-K_α (λ=1.54178 Å) line. Line profiles were recorded in a step-scanning regime with $\Delta(2\theta)=0.05°$. The temperature dependence of the electrical resistance and I-V characteristics were recorded by introducing the samples in a nitrogen cryostat or a He closed cycle cryostat and contacting the probes with soft Ag wire. During the measurements the pressure in cryostat was below 10^{-4} Torr. Electrical properties were measured with a Keithley 2400 source-meter or a Philips X-Y recorder, in the temperature range allowed by the experimental setup.

Thermally stimulated current (TSC) analysis was performed after filling the traps by adequate illumination (700 nm light, for 15 min.) at 50 K.

3. Experimetnal results

3.1. Structure

As revealed by XRD spectra, the films consist of a hexagonal compact (hcp) wurtzite phase, which is known to be the stable one for this material. The films are preferentially oriented with (001) crystalline direction perpendicular to their surface. The position of the peaks yields hcp lattice constants of 4.296Å (a_h) and 7.030Å (c_h). While a_h is consistent with the reported bulk value, c_h is somewhat larger.

A simple inspection of the diffraction pattern shows that both broadened lines and sharp reflections are present. An explanation for this [12] has been given as due to faulting. In the case of crystals made up of close-packed layers of atoms, stacking faults (mistakes in the normal hexagonal or cubic packing order) may easily occur. The energy of producing such defects is very low. For reflections of the type (*hk*0), (00*l*) and (*hkl*) with $h=k=3n$, there is no change in structure factor on crossing the fault, therefore no broadening is observed. In contrast, for (*hkl*) reflections with $h-k=3n\pm1$, the structure factor changes significantly at each fault, which results in broadening the line. The amount of broadening depends on the number of stacking faults.

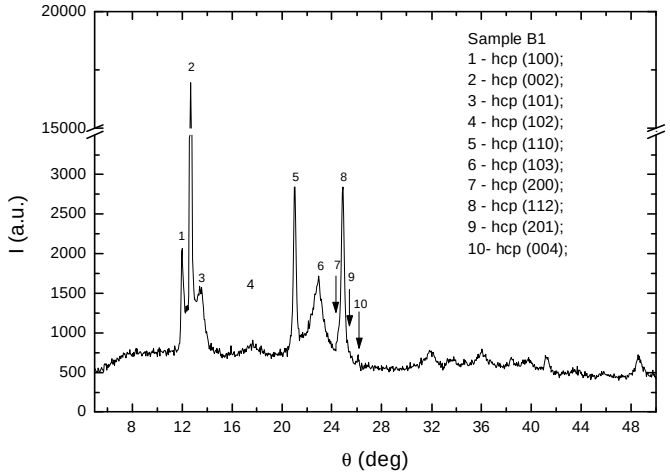

Fig. 1. Experimental X-ray diffraction pattern of a CdSe thin film sample.

The coherence lengths D_{eff}, calculated for three samples from (002) peak, are indicated in Table I. D_{eff} values were obtained using the well-known Scherrer formula:

$$D_{eff} = \frac{0.9\lambda}{\delta \cos\theta_0}, \tag{1}$$

where λ is the X-ray wavelength, θ_0 is the angle where the peak occurs and δ is its full width at half-maximum.

Table 1. Coherence length, as determined from (002) peak.

Sample	D_{eff} (Å)
B1	1072
B2	1352
B3	1587

Within the limits of experimental resolution, no change in diffraction pattern aspect or in line broadening was observed following electron irradiation at fluences up to 10^{16} electrons/cm^2 (Fig. 2). Therefore there are no major changes in the crystalline structure of the films, as a result of electron irradiation at energy and fluences indicated above. It may be concluded that at most point-like defects (vacancies, interstitials or their association in some more complex defects) do occur in the structure of the films.

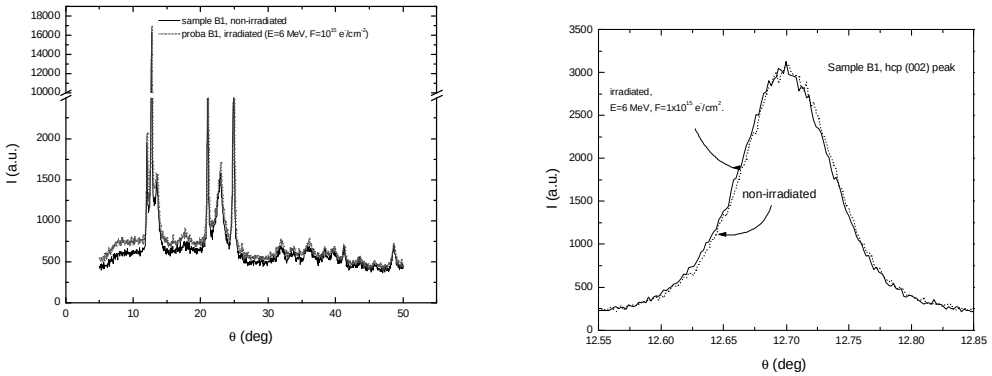

Fig. 2. X-ray diffraction pattern and hcp (002) peak for sample B1, before and after irradiation.

3.2. Electrical properties

3.2.1. Au/CdSe/Au sandwich cells

The current-voltage characteristics of the Au/CdSe/Au cells, before and after the two sessions of irradiation, are nonlinear and completely symmetrical with respect to the polarity of applied voltage. The Ohm's law is followed at low applied voltage, with a thermally activated conductivity. The temperature dependence of the electrical conductivity is well described by the expression:

$$\sigma(T) = \sigma_1 \exp\left(-\frac{E_{a1}}{k_B T}\right) + \sigma_2 \exp\left(-\frac{E_{a2}}{k_B T}\right), \tag{2}$$

as demonstrated by the plot in Fig.3. The values of the parameters entering eq. (2), as obtained by numerical fit, are indicated in Table 2. The experimental results suggest that there are two competing conduction mechanisms: one of them, with larger activation energy and dominating in the high temperature range, implying carriers in extended band states (conduction band mechanism), the other involving the hopping of the charge carriers over localized states induced by the structural and/or chemical disorder in the bandgap, dominating at low temperatures . The values of σ_1 and E_{a1} in Table 2 correspond to the conduction band mechanism, while σ_2 and E_{a2} are typical for the hopping mechanism

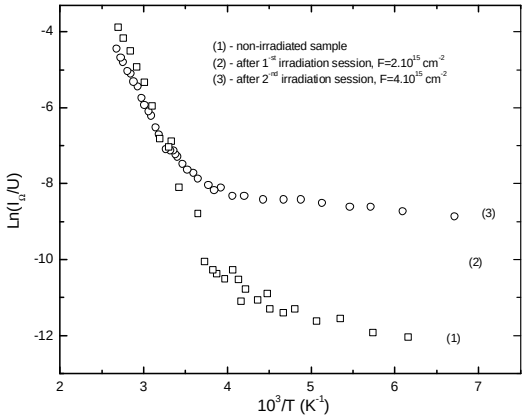

Fig. 3. Dependence of the electrical conductivity on reciprocal temperature, for the non-irradiated sample (1) and after two subsequent irradiation sessions with 7 MeV electrons to the fluences: 2×10^{15} cm^{-2} (2) and 4×10^{15} cm^{-2} (3), respectively.

Table 2. Parameters describing the electrical properties of the films and the defect band states.

	σ_1 ($\Omega^{-1}cm^{-1}$)	$E_{a1}=E_c-E_{F0}$ (eV)	σ_2 ($\Omega^{-1}cm^{-1}$)	E_{a2} (eV)	N_0 ($cm^{-3}eV^{-1}$)	$\|E_0\|$ (eV)	ΔE (eV)
before irradiation	514.17	0.46	4.59×10^{-6}	0.048	1.09×10^{14}	0.41	0.055
after 1^{-st} irradiation	91.44	0.42	8.54×10^{-6}	0.018	3.31×10^{14}	0.41	0.052
after 2^{-nd} irradiation	11.47	0.37	4.69×10^{-6}	0.029	5.74×10^{14}	0.41	0.052

After irradiation a shift of the Fermi level towards the conduction band (CB) was observed, as well as an important decrease of the pre-exponential factor σ_1. The Fermi level is pinned by some defect states of donor type, whose density is strongly affected by irradiation. Using the measured values of E_{a1} and E_{a2}, the location of these defect states in the band gap of CdSe can be determined with the following argument. The hopping activation energy E_{a2} is roughly of the order of $|E_0 - E_{F0}|$, where E_0 is the energetic separation between the center of the band of defect states and the bottom of CB E_c, and E_{F0} is the equilibrium Fermi level, also measured from E_c [13]. In the following all energetic values will be considered with respect to E_c, taken as the zero on energy scale (so E_0 , $E_{F0}<0$). If $E_0 > E_{F0}$ (the center of defect band located between the Fermi level and the bottom of CB), states lying near the Fermi level are very rare, their overlap is weak, and consequently their contribution to the hopping conductivity can be neglected. The main contribution to hopping conduction is due to electrons activated from the Fermi level into the peak of the density of states, so $E_{a2} = E_0 - E_{F0}$, or equivalently, $E_{a2} = E_{a1} - |E_0|$ (see Fig. 4). The same argument holds for the case where $E_0 < E_{F0}$ (the Fermi level located between the center of defect band and the bottom of CB), when the hopping conduction is mainly associated with the motion of the holes over defect states whose energy is close to E_0, and $E_{a2} = E_{F0} - E_0$. This seems to be the case after the second irradiation. Comparing the values of E_{a2} and E_{a1} in Table II, a value E_0 of about -0.41 eV is obtained. The locations of the defect band and of the Fermi level before and after irradiation are indicated in Fig. 4.

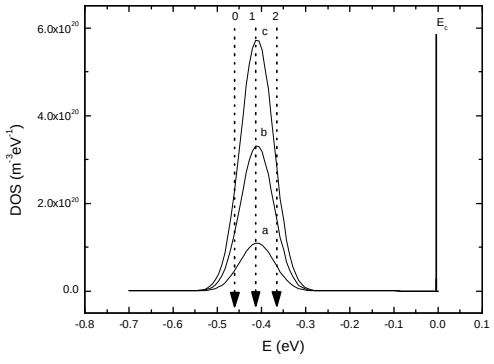

Fig. 4. Model of defect states band in the band gap of CdSe, as suggested by the analysis of the presented transport data. The irradiation influence on the location of the Fermi level (0- non-irradiated, 1-after first and 2- after the second irradiation) and also on the defect states density (a- non-irradiated, b-after first and c- after the second irradiation) are indicated.

Further insight on the effect of irradiation can be achieved by examining the super-linear region of the I-V characteristics. We interpreted the data in that range, in the frame of space-charge limited currents (SCLC) theory. Accordingly, for a *n*-type material, the electric field $E(x)$ in the sample is given by the Poisson equation [14]:

$$\frac{dE}{dx} = \frac{e}{\varepsilon_0 \varepsilon_r} \cdot (n - n_0 + n_t - n_{t0}), \quad E(0) = 0, \tag{3}$$

and the current density, constant through the sample, is:

$$j = e\mu_n n(x)E(x) = \text{const.} \tag{4}$$

In eq. (3) $n_0 = N_c \, exp\left(\frac{E_{F0} - E_c}{k_B T}\right)$ and n_{t0} are the thermal equilibrium free and trapped carrier density, $n = N_c \, exp\left(\frac{E_F - E_c}{k_B T}\right)$ and n_t denote the same quantities in the non-equilibrium case, when the carrier injection at the contacts becomes important, $\varepsilon_0 = 8.85 \times 10^{-12}$ F/m is the vacuum permitivity, $\varepsilon_r = 10$ is the CdSe dielectric constant[14], e is the electron charge, E_{F0} is the equilibrium Fermi level given in Table II, E_F is the non-equilibrium quasi-Fermi level. Considering the effective mass of electrons in CdSe, $m_n = 0.13 \cdot m_0$, the effective density of states in the conduction band was evaluated as $N_c = 2\left(\frac{2\pi m_n k_B T}{h^2}\right)^{3/2} = 0.226 \cdot 10^{21} T^{3/2}$ m^{-3}. Assuming a set of traps distributed in energy, having some density of states $N_t(E)$, n_t can be written as:

$$n_t = \int_{E_v}^{E_c} \frac{N_t(E)dE}{1 + \frac{1}{2} exp\left(\frac{E - E_F}{k_B T}\right)} = \int_{E_v}^{E_c} \frac{N_t(E)dE}{1 + \frac{n_0}{2n} exp\left(\frac{E - E_{F0}}{k_B T}\right)} \quad . \tag{5}$$

The same expression holds for n_{t0}, with E_F replaced by E_{F0}. Using eqs. (3-5), the electrical field in the sample and, subsequently, the voltage across the sample, corresponding to each value of the current density can be calculated, if the analytical function $N_t(E)$ is known.

In order to interpret the data, we considered a defect band with a Gaussian shape, lying in the vicinity of the Fermi level:

$$N_t(E) = N_0 \, exp\left(-\left(\frac{E - E_0}{\Delta E}\right)^2\right). \tag{6}$$

A numerical fit procedure was developped for determining the parameters N_0, E_0 and ΔE entering eq. (6). The center of the defect band E_0 was restricted to 0.41 eV below the bottom of the conduction band, following the argument presented above. The I-V characteristics recorded at different temperatures were used (see Fig. 5), the parameters were determined for each of them and the average results are indicated in Table II. For the sake of simplicity only three I-V plots together with the corresponding results of the numerical fit were showed in Fig.5. For comparation purposes the characteristics recorded at about the same temperatures, for non-irradiated and irradiated structures, have been chosen.

As expected, an increase of the defect state density from 1.09×10^{14} cm^{-3}eV^{-1} for the non-irradiated sample to 5.74×10^{14} cm^{-3}eV^{-1} after the second session of irradiation was observed. There is no significant change of the width ΔE=0.11 eV of the defect band.

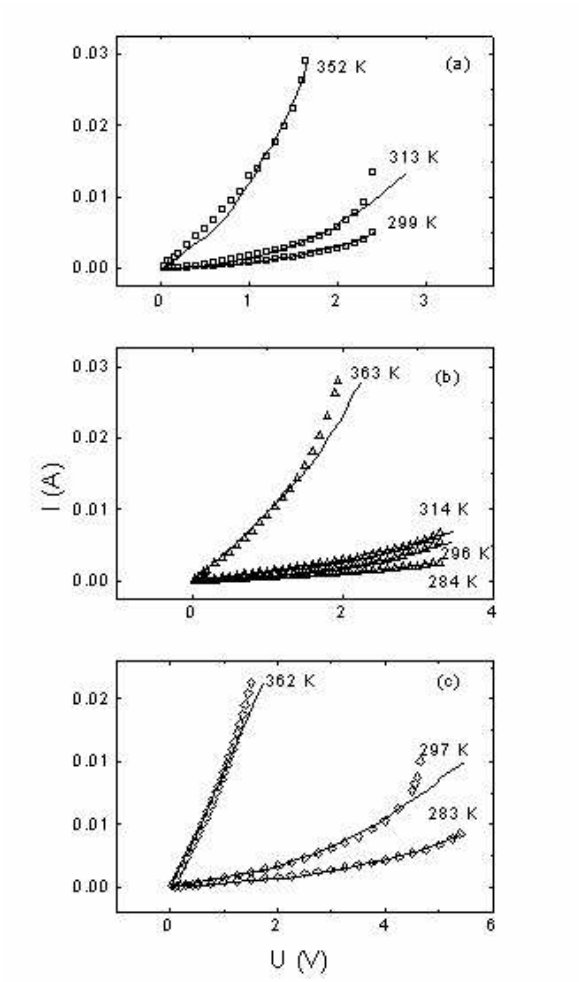

Fig. 5. Current-voltage characteristics at different temperatures, before (a) and after the first (b) and second (c) irradiation sessions. Both the measured values (points) and the best fits (continuous line) obtained as indicated in text are plotted.

3.2.2. Planar structures

The Arrhenius plot of the measured electrical resistance is shown in Fig. 6. One can easily observe that electron irradiation (6 MeV electrons to a fluency of 5×10^{13} electrons/cm^2) induced only slight changes in electrical properties, except for temperatures below 90 K. In some temperature ranges, the temperature dependence of the films resistance is well described by:

$$R(T) = R_0(T)\exp\left(\frac{E_a}{k_B T}\right) \tag{7}$$

where E_a is the activation energy. The pre-exponential factor R_0 may have a slight temperature dependence, reflecting, for example, the temperature dependence of free carriers mobility in the case of band conduction mechanism. Table III presents the values of E_a and R_0 parameters appearing in eq. (7), as obtained by numerical fit in the indicated temperature ranges. A band conduction mechanism is responsible for the observed electrical properties at room temperature and down to 240 K, controlled essentially by a deep donor level (D_1) located at 0.37 eV below the bottom edge of the conduction band. In this region the temperature dependence of the electrical resistance is entirely

due to the rapid decrease in the concentration of the free carriers (electrons), gradually recaptured by the donor levels they originate from. An increase of the pre-exponential parameter, R_0, was observed after irradiation, which can be explained by the increase of the density of defect states in the films, and the corresponding decrease of the mobility of the free carriers.

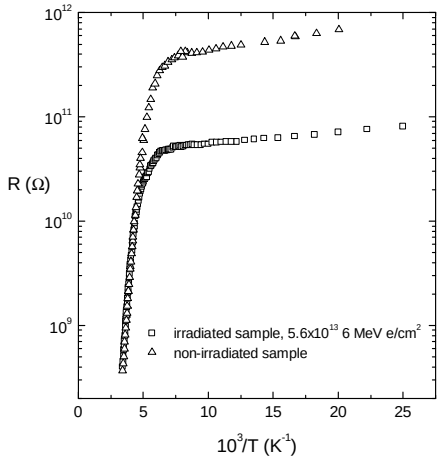

Fig. 6. Temperature dependence of the electrical resistance of the films, before and after irradiation with 6 MeV, 5×10^{13} electrons/cm^2.

One can easily observe more significant changes after irradiation in the low temperature range, below 90 K (Fig. 6). E_a and R_0 values in this range, as well as the effect of irradiation, can be explained assuming that the electrical conduction comes from electrons hopping between D_1 donor states, partially emptied by compensation. Unlike the room temperature case, the pre-exponential factor R_0 drops by almost an order of magnitude after irradiation. This is typical for hopping conduction mechanism, when R_0 depends exponentially on the density of localized states involved in the process [13].

Table 3. Parameters characterizing the electrical resistance (eq. (7)), as obtained by numerical fit.

Temperature range (K)	E_a (eV)	R_0 (Ω)	Obs.
300-240	0.37	165.5	as grown sample
	0.37	248.8	irradiated sample
100-40	0.004	2.84×10^{11}	as grown sample
	0.003	3.87×10^{10}	irradiated sample

TSC spectra analysis, performed both before and after irradiation, allowed us to obtain a more detailed quantitative information on the effect of electron irradiation on the films. A well resolved TSC peak, originating from thermal release of charge carriers from a trap having activation energy E_{t0} into conduction or valence band, is described by [15]:

$$I_{TSC}(T) = I_0 \exp\left(-\int_{T_0}^{T} \frac{e_t}{\beta} dT'\right), \tag{8}$$

where $I_0 = Ce\mu\tau N_t e_t V$, e is the electron charge, μ and τ are, respectively, the mobility and lifetime of free carriers, V is the applied voltage, C is a geometrical, N_t is the trap density, T_0 is the starting temperature, β is the heating rate and e_t is the emission rate from the trap, given by:

$$e_t = \frac{16\pi m^* k_B^2}{h^3} \sigma_t T^2 \exp\left(-\frac{E_{t0}}{k_B T}\right). \tag{9}$$

In eq. (9) m^* is the free carrier effective mass, h is Planck's constant, k_B is Boltzmann's constant, σ_t is the free carrier capture cross-section and E_{t0} is the ionization energy of the traps. Usually, the temperature dependence of σ_t can be expressed as $\sigma_t = \sigma_{t0}\exp\left(-E_\sigma / k_B T\right)$ and the experimentally measured trap activation energy is then $E_t = E_{t0} + E_\sigma$.

It was shown [16,17] that the integral in eq. (8) can be approximated to the following, more practical, result:

$$I_{TSC}(T) = I_0 \exp\left\{-\frac{E_t}{k_B T} - \frac{k_B D_t}{\beta E_t} T^4 e^{-E_t/k_B T} \times \left[1 - 4\frac{k_B T}{E_t} + 20\left(\frac{k_B T}{E_t}\right)^2\right]\right\} \tag{10}$$

where $D_t = 2.95\times10^{21}(m^*/m_0)\sigma_{t0}$, with σ_{t0} in cm^2, m_0 is the electron rest mass, the numerical factor represents the constants entering eq. (8) and $I_0 = Ce\mu\tau N_t D_t T^2 V$.

Figure 7 shows the normalized TSC spectra measured before and, after irradiation, respectively. We have used the normalization procedure, introduced previously by Look et al., [18,19]. This procedure is based on the observation that both TSC and photocurrent I_{PC} are proportional to lifetime τ and mobility μ of the carriers, and therefore, their ratio I_{TSC}/I_{PC} should only depend on quantities that can be obtained by fit. In this way complete quantitative results can be extracted from TSC data. In case of thin films ($\alpha d << 1$, α being light absorption coefficient and d the film thickness), the photocurrent is given by $I_{PC} = Ce\mu\tau\Phi_0\alpha V$, where Φ_0 is the incident light flux and C the geometrical factor entering eq. (8). The I_{TSC}/I_{PC} ratio is then given by:

$$\frac{I_{TSC}}{I_{PC}} = \frac{N_t D_t T^2}{\Phi_0 \alpha} exp\left\{-\frac{E_t}{k_B T} - \frac{k_B D_t}{\beta E_t} T^4 e^{-E_t/k_B T}\left[1 - 4\frac{k_B T}{E_t} + 20\left(\frac{k_B T}{E_t}\right)^2\right]\right\}. \tag{11}$$

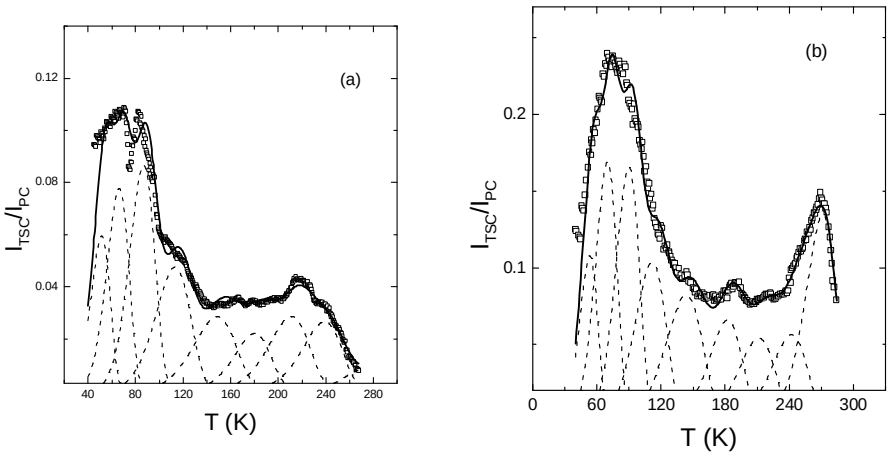

Fig. 7. Normalized TSC spectra, recorded before (a) and after (b) irradiation with 6 MeV, 5×10^{13} electrons/cm^2. Continuous lines represent the calculated TSC spectra by simultaneous fitting, while dashed lines indicate individual TSC peaks.

Both spectra consist of several heavily overlapped peaks and a direct use of eq. (11) for any of them is not adequate. To reduce the interference of neighboring peaks, a fractional heating technique was used: after illumination the sample was heated with constant rate to a temperature

3-5 K larger than that corresponding to a maximum or shoulder in TSC spectrum, it was maintained at that value for 5 min., then the sample was cooled down to a temperature 30 K lower and the cycle was repeated. It is expected that by such a procedure shallower levels are gradually emptied and their influence on the deeper ones reduced. However, some peaks are to close to each other to be experimentally resolved, even by fractional heating, and a simultaneous fit with two features described by eq. (11) had to be performed, especially for the low temperature region.
The values of the parameters E_t, σ_{t0}, and I_0 obtained at this stage were then used as initial guess for a simultaneous fit of the spectra with sums of features given by eq. (11). In Ref. 17 it was demonstrated that this procedure minimizes errors in parameters of each peak and can indicate "missing" peaks. After this step E_t and σ_{t0} values remained practically unchanged, while pre-exponential factors I_0 were modified. This was to be expected, since the repeated heating-cooling cycle modifies the initial concentrations of trapped electrons for peaks corresponding to deeper levels overlapping with analyzed ones. The trap parameters, as obtained by this procedure, are indicated in Table 4.

Table 4. Parameters of the trapping levels in CdSe thin films, before and after 6-MeV accelerated electron-irradiation to the fluency 5×10^{13}, electrons/cm^2.

Trap	E_a (eV)	N_t (cm^{-3}) [a]	N_t (cm^{-3}) [b]	σ_{t0} (cm^2)
D_1	0.38	4.79×10^{13}	7.70×10^{14}	4.9×10^{-13}
D_2	0.24	7.22×10^{13}	1.58×10^{14}	4.5×10^{-15}
D_3	0.17	4.31×10^{13}	8.23×10^{13}	5.8×10^{-16}
D_4	0.14	1.93×10^{13}	5.97×10^{13}	4.3×10^{-16}
D_5	0.06	1.03×10^{13}	2.68×10^{13}	6.2×10^{-18}
D_6	0.04	7.70×10^{12}	1.62×10^{13}	4.6×10^{-18}
D_7	0.036	6.20×10^{12}	1.33×10^{13}	2.3×10^{-17}
D_8	0.02	2.71×10^{12}	7.25×10^{12}	7.3×10^{-18}
D_9	0.01	1.20×10^{12}	2.51×10^{12}	3.1×10^{-18}

[a] as grown sample; [b] irradiated sample

The most important effect of electron irradiation is easily seen in the high temperature region of the spectra. The density of D_1 traps is larger by more than an order of magnitude after irradiation, also an important increase of D_4 traps density is evident.

4. Discussion

The experimental results obtained by various methods converged to the conclusion that electrical properties of the films prepared as described above are controlled by a main donor defect located at 0.38-0.40 eV below the conduction band. The results also clearly demonstrated that the density of those defect centers is significantly increased by irradiation with electrons having energies in MeV range.

It is difficult to establish the origin of defects identified by the above-indicated experimental procedures. This task is further complicated in the case of thin films, where local structural disorder exists at grain boundaries or surface and can lead to a broadening of otherwise well defined levels. However, the simplest defects presumably to act as deep donors in CdSe are Se-vacancies and Cd-interstitials. Such defects are also very likely to be produced by electron irradiation. The peculiarity of irradiation with high-energy (in MeV range) electrons consists in the fact that it produces a few atomic displacements. The maximum energy transferred at impact by an electron having an energy E to an atom of mass M is given by [20]:

$$E_m = 2\frac{m_0}{M}E\left(2+\frac{E}{m_0c^2}\right). \qquad (12)$$

For an initially 6 MeV electron, the maximum energy transferred to a Cd atom is 802 eV, while for a Se atom it is 1140 eV. The exact threshold energy for atomic displacement in CdSe is unknown, to our knowledge. For other compound semiconductors, experimentally determined threshold energy ranges from about 6 eV to 12 eV (Ref. 20, p. 229). A value of 8.7 eV was measured in the case of a related compound, CdS (Ref. 9, p. 194). Assuming a displacement energy of 10 eV, each primarily knock-on atom can produce up to 50 secondary displacements. The rate of energy loss of incident electrons is of the order of 10 MeV/cm [9] and consequently the electron energy loss in our samples is negligible, which implies that the irradiation generated Frenkel (interstitial-vacancy) pairs are uniformly distributed in volume. Some of them disappear by direct recombination. But it is plausible that interstitials, having larger mobility than vacancies, will more easily migrate among vacancies, eventually being trapped by other defects at surface or grain boundaries. Consequently, some of the vacancies produced by electron irradiation will survive the recombination process. They could also form aggregates and/or interact with oxygen atoms residually present in the vacuum chamber. We infer that D_1 defect, which is determining electrical properties of our samples and is predominantly produced by irradiation, may be assigned to a Se-vacancy or a more complex point-like defect associated to a Se-vacancy.

5. Conclusions

We presented in this paper an investigation by various techniques on the effects of 6 MeV electron irradiation on electrical properties of CdSe thin films grown by vacuum deposition.

XRD spectra revealed that the films consist of hcp wurtzite phase, preferentially oriented with (001) crystalline direction perpendicular to their surface. Within the limits of experimental resolution, no change in diffraction pattern aspect or in line broadening was observed following electron irradiation at fluences up to 10^{16} electrons/cm^2. It follows then that irradiation with 6-MeV electrons results in the creation of point-like defects.

Electrical properties of the films were investigated using two different geometries, Au/CdSe/Au sandwich cells and, respectively, planar structures with four Al contacts deposited on top of the films. A model was developed in the frame of SCLC theory with a more realistic energetic distribution of traps. This model was used to the analysis of experimentally obtained I-V curves for Au/CdSe/Au sandwich cells. The results are in perfect agreement with those obtained from TSC curves measured in the case o planar structures.

An extrinsic conduction determined by the presence of a main donor center located at 0.38-0.40 eV below the conduction band bottom edge was observed in the high temperature range (room temperature and below, to 240 K). At low temperatures charge transport occurs through hopping mechanism; in that temperature range the effect of irradiation is more pronounced. The density of localized states involved in the hopping process is increased by irradiation, consequently the overlap of their corresponding wave functions increases, which results in exponentially smaller resistance values.

From TSC spectra analysis, several traps were identified in the band gap. The above mentioned deep donor D_1 with ionization energy of 0.38 eV, which mainly controls electrical behavior of the films, exists in larger densities. The TSC procedure we used allows for an accurate determination of trap parameters. After irradiation a significant increase of D_1 trap density occurred. We believe that D_1 is related to a Se-vacancy or to a more complex defect associated with a Se-vacancy. The origin of the other identified defects, with smaller ionization energies, remains unknown at this time.

References

[1] G. Jäniche, H. Berger, J. Vac. Sci. Tech. **6**, 552 (1969)
[2] H. Berger, G. Jäniche, N. Grachovskaya, phys. status solidi **33**, 417 (1969).
[3] R. Bube, L. Barton, J. Chem. Phys. **29**, 128 (1958).
[4] K. Shimizu, Japan. J. Appl. Phys. **4**, 627 (1965).

[5] V. Ruxandra**,** S. Antohe, J. Appl. Phys. **84**, 727-733, (1998)
[6] S. Antohe, L. Ion, V. Ruxandra, J. Appl. Phys. **90**, 5928 (2001).
[7] S. Antohe**,** L. Ion, V. A. Antohe, J. Optoel. Adv. Mat. **5** (4) 801-816 (2003).
[8] L. Ion, S. Antohe , M. Popescu, F. Scarlat, F. Sava and Felicia Ionescu, J. Optoelectron. Adv. Mater. **6**(1), 113 (2004).
[9] J. W. Corbett, "Electron Radiation Damage in Semiconductors and Metals" (Solid State Physics Series, Vol. 7(suppl.), Academic, New York, 1966).
[10] J. Dresner and F. V. Shallcross, J. Appl. Phys. **34**, 2391 (1963).
[11] V. Ruxandra, J. Mater. Sci. Lett. **16**, 1833 (1997).
[12] E. F. Kaelble (ed.), "Handbook of X-Rays", chapt. 17, McGraw-Hill, New York, USA, 1967.
[13] B. I. Shklovskii, A. L. Efros, "Electronic Properties of Doped Semiconductors" (Springer, Berlin, 1984), chapt. 6.
[14] M. A. Lampert, P. Mark, "Current Injection in Solids" (Academic Press, New York, 1970), pp. 33-38.
[15] D. C. Look, in Semiconductors and Semimetals, edited by R.K. Willardson and A.C. Beer, (Academic, New York, 1983), Vol. 19, p. 75.
[16] B. Santič, N. Radič, U.V. Desnica, Solid State Commun., **79**, 535 (1991).
[17] M. Pavlovič, U.V. Desnica, J. Appl. Phys., **84**, 2018 (1998).
[18] D. C. Look et al., Phys. Rev. **B55**, 2214 (1997).
[19] Z-Q. Fang, D. C. Look, Appl. Phys. Lett., **59**, 48 (1991).
[20] J. Bourgoin, M. Lannoo, "Point Defects in Semiconductors" II (Solid State Sciences Series, Vol. 35, Springer, Berlin, 1983), chapt. 8.